



## The role of the secondary fluorophore in ternary plastic scintillators aiming at discriminating fast neutrons from gamma-rays

Eva Montbarbon, Zhengyu Zhang, Amélie Grabowski, Romuald Woo,  
Dominique Tromson, Chrystèle Dehé-Pittance, Robert Bernard Pansu,  
Guillaume H. V. Bertrand, Matthieu Hamel

### ► To cite this version:

Eva Montbarbon, Zhengyu Zhang, Amélie Grabowski, Romuald Woo, Dominique Tromson, et al.. The role of the secondary fluorophore in ternary plastic scintillators aiming at discriminating fast neutrons from gamma-rays. *Journal of Luminescence*, 2019, 213, pp.67-74. 10.1016/j.jlumin.2019.04.059 . hal-02325687

**HAL Id: hal-02325687**

**<https://hal.science/hal-02325687>**

Submitted on 23 Oct 2019

**HAL** is a multi-disciplinary open access archive for the deposit and dissemination of scientific research documents, whether they are published or not. The documents may come from teaching and research institutions in France or abroad, or from public or private research centers.

L'archive ouverte pluridisciplinaire **HAL**, est destinée au dépôt et à la diffusion de documents scientifiques de niveau recherche, publiés ou non, émanant des établissements d'enseignement et de recherche français ou étrangers, des laboratoires publics ou privés.

# The role of the secondary fluorophore in ternary plastic scintillators aiming at discriminating fast neutrons from gamma-rays

Eva Montbarbon<sup>a, b</sup>, Zhengyu Zhang<sup>b</sup>, Amélie Grabowski<sup>a</sup>, Romuald Woo<sup>a</sup>, Dominique Tromson<sup>a</sup>,  
Chrystèle Dehé-Pittance<sup>a</sup>, Robert B. Pansu<sup>b</sup>, Guillaume H. V. Bertrand<sup>a</sup>, Matthieu Hamel<sup>a, \*</sup>

<sup>a</sup> CEA, LIST, Laboratoire Capteurs et Architectures Électroniques, F-91191 Gif-sur-Yvette Cedex, France.

<sup>b</sup> ENS Paris Saclay, UMR CNRS 8531, F-94235 Cachan, France.

## Abstract

Since Helium-3 shortage announcement, organic scintillators play a major role in neutron detection. Our laboratory decided to focus on plastic scintillators and their ability to discriminate fast neutrons from gamma rays. In this work, we highlight the influence of the secondary fluorophore in lab-made plastic scintillators. The secondary fluorophore is generally added in the scintillating mixture to shift the emission wavelength towards the transparency domain of the material to improve its attenuation length. Thus, it is considered as a harmless molecule and is barely seen as a key criterion that could enhance the performances of the organic scintillator. In our work, we demonstrate that this molecule, even added at a small concentration (typically in the range 0.02 – 0.2 wt%), directly impacts the neutron/gamma discrimination ability of plastics. Not only the secondary fluorophore plays a role in self-absorption of the scintillating material, but also the couple it creates with the primary fluorophore has to be carefully chosen, as some specific triplet energy transfers between the two fluorophores can influence the neutron/gamma discrimination abilities of the plastic scintillator. Aside from classical photophysical inconveniences such as self-absorption or diffusion, the possibility that the whole, bulk material was heterogeneous in a photochemical point of view was also checked. Thus, various samples were cut from bulk monoliths and their pulse shape discrimination compared with the parent scintillator in terms of Figure of Merit and light output.

## Keywords

n/γ discrimination; plastic scintillators; secondary fluorophore; self-absorption; triplet-triplet annihilation.

## Highlights

- Fast neutrons/gamma discrimination efficiency is usually reduced when the volume of a plastic scintillator is increased.
- This effect is studied, first in a morphologically way, then chemically and photophysically.

## I. INTRODUCTION

Protection of civilians and facilities against CBRN-E threats (“Chemical, Biological, Radiological, Nuclear, and Explosive” threats) has become a true challenge these last fifteen years. In the context of nuclear and radiological threats, Helium-3 based counters have proven their efficiency and are considered as the “Gold standard” in neutron detection. These historical detectors are widely used in Radiation Portal Monitors (RPMs) which are installed, *e.g.*, at borders and tolls. However, the shortage of Helium-3 production which occurred for years have incited many scientists to imagine reliable and potentially cheaper alternatives.<sup>1,2</sup>

In this situation, organic scintillators may pave the way to a new paradigm in neutron detection. Indeed, some scintillators were chemically engineered for Pulse Shape Discrimination (PSD), and especially the discrimination between fast neutrons and gamma rays, which falls within nuclear and radiological detection.<sup>3</sup> Organic crystals are among the best performing materials to discriminate fast neutrons from gamma rays but are constrained to high-price, small-scale samples. Contrary to crystals, liquid and plastic scintillators have the benefit of being cheap, scalable to sizes fully compatible with sensors encountered in RPMs and easy to manufacture. Thus, they could be suitable to replace <sup>3</sup>He counters, owing to the fact they are good enough to meet normative neutron detection requirements. A plastic scintillator is generally made out of a polymer matrix, a primary and a secondary fluorophore. The first fluorophore collects the singlet and triplets produced by the ionizing particle in the material. Its concentration is chosen to allow the presence of a delayed fluorescence from triplet-triplet annihilation (TTA). This TTA probability is higher in the case of fast neutrons compared to gamma rays. The secondary fluorophore absorbs the first fluorophore’s emission and acts as a “wavelength shifter” by emitting light at wavelengths that are in the transparency domain of the plastic scintillator, and for

which the photon to electron conversion is the highest according to standard photocathodes used in photomultiplier tubes (most of the time  $\lambda \approx 420$  nm).

Generally, the secondary fluorophore is mainly being considered as a wavelength shifter. The nature of the molecule and its concentration is not considered to influence *a priori* the neutron/gamma discrimination abilities of the plastic scintillator in which it is incorporated. The results described herein show that this postulate must be reconsidered. Our aim is to analyze the main photophysical phenomena of the discrimination between fast neutrons and gamma rays in plastic scintillators, and especially the role of the secondary fluorophore in this process. For this purpose, different experiments have been carried out and are presented in the following.

For this purpose, the influence of the secondary fluorophore was demonstrated towards the performances of the scintillator, and the photophysical processes involving this molecule were evidenced. The first experiment consisted in highlighting the influence of the secondary fluorophore on the neutron/gamma discrimination properties. In this purpose, a set of eight plastic scintillators of the same volume has been synthesized. Four different secondary fluorophores were tested: bis-methylstyrylbenzene (bis-MSB), 9,10-diphenylanthracene (9,10-DPA), 1,4-bis(5-phenyl-2-oxazolyl)benzene (POPOP) and 1,4-bis-2-(4-methyl-5-phenyloxazolyl)benzene (diMePOPOP). The scintillators were intentionally prepared in pairs, the weight concentration of the introduced secondary fluorophore being either 0.1 or 0.2 wt%. The results of the eight plastic samples were presented in terms of FoM, scintillation decay time and relative intensities. The FoM was evaluated thanks to Equation 1, where  $\mu_n$  and  $\mu_\gamma$  are the mean positions of the neutron and the gamma ray contributions, and  $\sigma_n$  and  $\sigma_\gamma$  are the standard deviations of neutron and gamma lobes:

Equation 1

$$FoM = \frac{|\mu_n - \mu_\gamma|}{2.35(\sigma_n^2 + \sigma_\gamma^2)}$$

The next experiment consisted in slide-cutting two of these plastic samples, centimeter by centimeter. In this way, we could evaluate the Figure of Merit value (FoM) as a function of the length of the plastic material.

In addition, experiments related with the homogeneity of large or long PSD-plastic were conducted, where portions were randomly isolated from bulk scintillators. The obtained results enabled us to propose two assumptions of the FoM differences we notice: the formation of exciplexes in the sample, or triplet energy transfers between the primary and the secondary fluorophores. The last part of this paper describes experiments we carried out to verify these hypotheses. Finally, conclusions about photophysical phenomena were drawn.

Since the 70's, almost two decades after the discovery of plastic scintillators, it has been observed that the observed light yield and the discriminating abilities of organic scintillators decrease when the

volume increases. For instance, Kalyna and Taylor carried out fast neutrons/gamma rays discrimination experiments with liquid scintillators of different diameter but with a constant height, which was stand equal to 1 inch.<sup>4</sup> The authors observe that the FoM of a 4'' Ø NE213 liquid scintillator is equal to 1.75, whereas it only reaches 0.9 when its diameter is doubled. According to them, this difference of FoM value is mainly due to the high voltage of the photomultiplier tube (PMT) which is applied, and has to be adjusted according to the dimensions of the scintillator. Sipp and Miehe compare the radioluminescence decays of BIBUQ-based fluorescent solutions (BIBUQ stands for 4,4'-bis-(2-butyl-octyloxy)-*p*-quaterphenyl), in which 56 g.L<sup>-1</sup> BIBUQ is incorporated in xylene.<sup>5</sup> 0.2, 1 and 5 cm-long optical length cuvettes are thus being compared. A sum of two exponential functions is used to fit the measured decay times. The prompt decay of these liquid scintillators, which is relative to fast fluorescence, varies very slightly from one solution to another. However, the Full Width at Half Maximum (FWHM) of the recorded pulses increases from 1.58 ns up to 2.28 ns when the optical length cuvette is increased from 0.2 cm up to 5 cm. According to Sipp and Miehe, this time difference is due to an absorption phenomenon, where scintillation photons are self-absorbed by the material and reemitted with a second delay. Moszyński *et al.* evaluated the neutron/gamma discrimination abilities of NE213 with different volumes. With their detection setup, they notice that the FoM is equal to 1.58 at 300 keVee for this liquid scintillator when its dimensions are 16 cm diameter and 20 cm height, whereas the FoM reaches 2.61 when the same scintillator measures 5 cm diameter and 5 cm height.<sup>6</sup> In conclusion, the authors explain this loss of luminous and discriminating signals of organic materials by self-absorption. As the PSD is based on very subtle differences in the decay time distributions between a gamma and a neutron interaction within the material, self-absorption phenomenon tends to fade out this small discrepancy. Recently, the impact of the secondary dye – both in terms of light output and FoM – was experimentally observed on neutron/gamma discriminating plastics, but not explained.<sup>7</sup> Also, the POPOP molecule suffered from important irradiation doses to give a derivative.<sup>8</sup> Despite the fact that the scintillator showed a degraded light output, the FoM value was improved. As a reminder, self-absorption is a molecular absorption phenomenon that takes place inside the scintillator: scintillation photons are emitted, possibly reabsorbed by the material, and then reemitted by secondary emission. Thus, the larger the volume, the more self-absorption may occur. In a ternary system, self-absorption is due to a spectral overlap between the absorption and the emission spectra of the last fluorophore, thus the secondary fluorophore. Besides, the Stokes shift quantifies this overlap. Equation 2 gives the formula of the Stokes shift  $\Delta\nu_{Stokes}$ :

Equation 2

$$\Delta\nu_{Stokes} = \nu_{abs} - \nu_{fluor} = 1/\lambda_{abs} - 1/\lambda_{fluor}$$

$\nu_{abs}$  and  $\nu_{fluor}$  are respectively the wavenumbers of absorbance and fluorescence (in  $\text{cm}^{-1}$ ). Providing the fact that the polymer would have an almost full transmission at the emission wavelength, a scintillator – and therefore its fluorophores – with a very large Stokes shift should virtually not display any self-absorption process. Thus, self-absorption depends on both the volume and the concentration of the secondary fluorophore in a ternary organic scintillator. To the best of our knowledge, only one article relates the dependence between the secondary fluorophore concentration with the volume. Adadurov *et al.* adjusted the weight percentage of the secondary fluorophore to the volume of the material.<sup>9</sup> Thanks to beta spectroscopy, the authors determined a relationship between scintillation efficiency and weight concentration of POPOP, used as the secondary fluorophore. Furthermore, they drew the weight concentration of the secondary fluorophore relative to the optical length. Our aim is to understand the influence of the secondary fluorophore in neutron/gamma discrimination process. According to the mentioned literature, self-absorption taking place in lab-made ternary systems could be a consequence of the choice of the secondary fluorophore and its concentration. Our strategy is to evaluate the neutron/gamma discrimination abilities of plastic scintillators of different sizes and various secondary fluorophores, incorporated at two weight concentrations. This would enable us to highlight the self-absorption phenomenon.

## II. EXPERIMENTAL

All the chemicals were purchased from Sigma-Aldrich and used as received unless otherwise stated. Styrene was vacuum-distilled over calcium hydride prior to the experiment and the inhibitors were removed from the cross-linker agent.

The general procedure for the plastic scintillator preparation is as follows: in a flame-dried round bottom flask filled with argon, the powders were dissolved in the liquids. The gases were then removed using the freeze-pump-thaw technique, and the solution was carefully transferred into a vial for radical polymerization. After completion, the vial was shattered with a mallet and the scintillator was obtained after shaping and polishing the raw material. The contours and back were ultimately covered with PTFE for better light collection through multiple diffusive reflections.

Pulse Shape Discrimination was performed by irradiating plastic scintillators with a  $^{252}\text{Cf}$  radioactive source, whose activity was 560 kBq at the time of measurement. The tested scintillator was coupled to the photocathode of a Hamamatsu H11284-MOD Photomultiplier Tube<sup>10</sup> with Rhodorsil RTV141A optical grease. The PMT was fed by a CAEN N1470 high voltage operating at -1500 V. The anode of the PMT was linked to a CAEN DT5743 digitizer, whose bandwidth, sampling rate and resolution are 500 MHz, 800 MS/s and 12 bits, respectively. The WaveCatcher software from CAEN was used to record 25,000 pulses (or 35,000 pulses in some cases) with an integration time equal to 1280 ns. The

charge comparison method was then applied off-line thanks to a Matlab lab-made algorithm. It calculates delayed and total areas under each pulse, displays the bi-dimensional diagram and evaluates the Figure of Merit.

Gamma spectra were recorded using the same setup experiment: the CAEN DT5743 electronic board connected to the Hamamatsu H11284-MOD Photomultiplier tube. A 9.75 MBq  $^{22}\text{Na}$  source was placed 2.5 cm away from the top of the plastic scintillator to be analyzed.

Liquid scintillators were contained in 3 cm<sup>3</sup> quartz cuvettes. The solvent was spectroscopic toluene, and 0.03 wt% secondary fluorophore (POPOP, dimethylPOPOP, 9,10-DPA or bis-MSB) was introduced. Fluorescence spectra were recorded at 90° from the excitation light (270 nm) with a Horiba Jobin Yvon Fluoromax-4P device, monitored with FluorEssence software.

### III. NATURE OF THE SECONDARY FLUOROPHORE AND ITS IMPACT ON NEUTRON/GAMMA DISCRIMINATION

#### 1. Experimental details

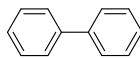
As already said in the introduction, a plastic scintillator is generally a ternary system. For the purpose of the studies, ternary plastic scintillators were lab-made according to a previous preparation.<sup>11</sup> The first series consists in eight plastic scintillators of 12 mm diameter and 120 mm height, thus giving a 14 cm<sup>3</sup> volume. The matrix and the primary fluorophore are identical: the matrix is a cross-linked polystyrene derivative and the weight concentration of the first solute (biphenyl) is 17 wt%. Four different secondary fluorophores were added as well to the scintillator mixture, with two different weight concentrations: 0.1 and 0.2 wt%, respectively. The list of lab-made scintillators is presented in Table 1, with the structure of the molecules in the Figure 1. The name of these plastics relies on the nature of the secondary fluorophore (in summarized form) and the weight concentration at which it is added.

Table 1. Lab-made plastic scintillators (Ø 12 mm × h 120 mm) prepared to study the influence of the nature of the secondary fluorophore

Scintillator	Secondary fluorophore	Concentration (wt%)
Bis1	Bis-MSB	0.1
Bis2	Bis-MSB	0.2
DPA1	9,10-DPA	0.1
DPA2	9,10-DPA	0.2
DMP1	DiMePOPOP	0.1
DMP2	DiMePOPOP	0.2
P1	POPOP	0.1

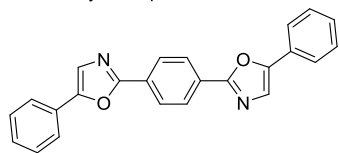
P2	POPOP	0.2
----	-------	-----

Primary fluorophore

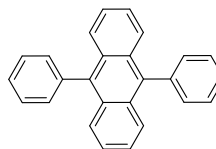


Biphenyl

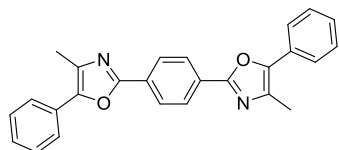
Secondary fluorophore



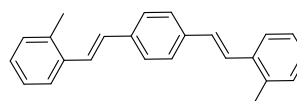
POPOP



9,10-diphenylanthracene



dimethylPOPOP



bis-methylstyrylbenzene

Figure 1. Chemical structures of biphenyl, 1,4-bis(5-phenyl-2-oxazolyl)benzene, 9,10-diphenylanthracene, 1,4-bis-2-(4-methyl-5-phenyloxazolyl)benzene and bis-methylstyrylbenzene.

The pulses assigned to neutrons were sorted, averaged and four photophysical criteria were evaluated thanks to the fitting module of the Igor Pro software: fast and slow decay times and their related intensities. Equation 3 displays the formula of the slow relative intensity, and Equation 4 shows the relationship between fast and slow relative intensities.

Equation 3

$$I_{rel,s} = \frac{A_{0s}\tau_s}{A_{0s}\tau_s + A_{0f}\tau_f}$$

Equation 4

$$I_{rel,s} + I_{rel,f} = 1$$

$A_{0f}$  and  $A_{0s}$  stand for fast and slow intensities at  $t = 0$  of the mean neutron signal, and  $\tau_f$  and  $\tau_s$  are the fast and slow decay times, respectively, which are convolved with the transit time of the PMT (equal to 29 ns according to the H11284-MOD PMT datasheet<sup>10</sup>).

Unlike commercial data sheets of organic scintillators that describe the decay time of a scintillator with three components,<sup>12</sup> we only evaluate fast and slow components of the signal. In fact, we consider that the fast component corresponds to prompt fluorescence – it is the decay rate of the fluorescence deactivation of singlet excited states – and the slow one represents delayed fluorescence, which is the radiative deactivation of the triplet excited states thanks to Triplet-Triplet Annihilation (TTA) mainly.

This photophysical phenomenon is the key step to explain fast neutron/gamma discrimination in such scintillators.<sup>13</sup>

## 2. Results

### 1) Self-absorption in 12 mm × 120 mm scintillators

Before testing all scintillators presented in Table 1, we focused on neutron/gamma discrimination abilities of DMP1 and DMP2 containing dimethylPOPOP as the secondary fluorophore. Our goal was to study and highlight self-absorption in these long and small plastic scintillators. Thus, plastics were irradiated with the <sup>252</sup>Cf radioactive source introduced above. We obtained FoM values thanks to signal processing. We then cut centimeter by centimeter both plastic materials and listed their FoM value after each removal. Results are showed in Figure 2.

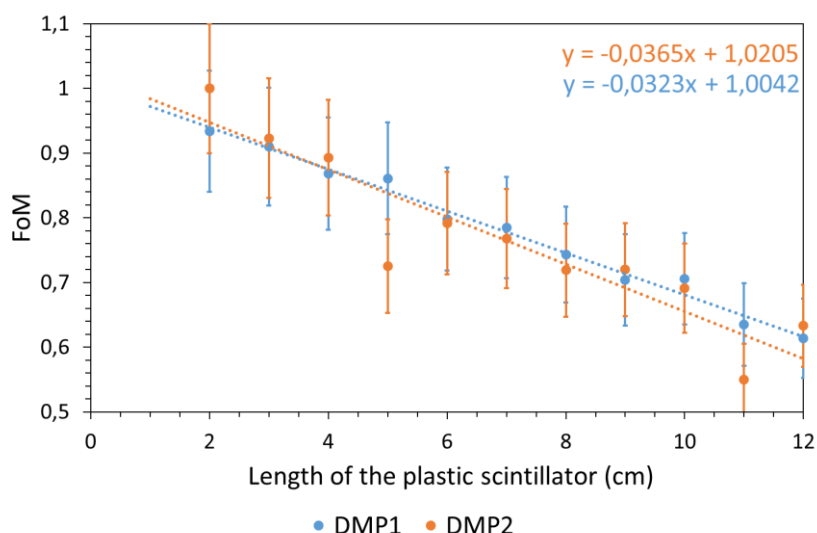


Figure 2. Evolution of FoM of DMP1 (0.1 wt% DiMePOPOP) and DMP2 (0.2 wt% DiMePOPOP) plastic scintillators along with the length of scintillators (note that these materials were not from the same batch as the ones tested in Table 1).

We noticed that the longer the samples, the smaller the FoM values. Furthermore, the FoM value is linearly proportional to the length of the plastic scintillator, whatever the weight concentration of the secondary fluorophore – at least in this study. The mean relative loss of FoM is around 55 %, so both plastic scintillators lose more than twice their neutron/gamma discrimination abilities from 2 to 12 cm long. Finally, linear fits, for which equations are written on Figure 2, indicate that the weight concentration of DiMePOPOP influences FoM as well.

In the case of POPOP, self-absorption of POPOP by the scintillator can be predicted from the absorption and fluorescence spectra of this molecule in the scintillator. On Figure 3 the absorption of a thin POPOP solution and the one of a 8.3 cm long scintillator are compared with the fluorescence of POPOP.

Whereas in solution only the first fluorescence peak at 382 nm is re-absorbed, in a thick scintillator the second peak at 408 nm is impacted. This has two consequences on the collection of fluorescence and on its apparent lifetime (Figure 4). The same PTFE-wrapped scintillator was excited with a 390 nm laser. Less than 10 % of the light produced 6 cm away from the head reached the detector. Due to multiple absorptions and re-emission, the apparent fluorescence decay time was increased by 50 %. We can thus qualitatively conclude that the self-absorption process can affect the FoM value in those long and small sized plastic scintillators.

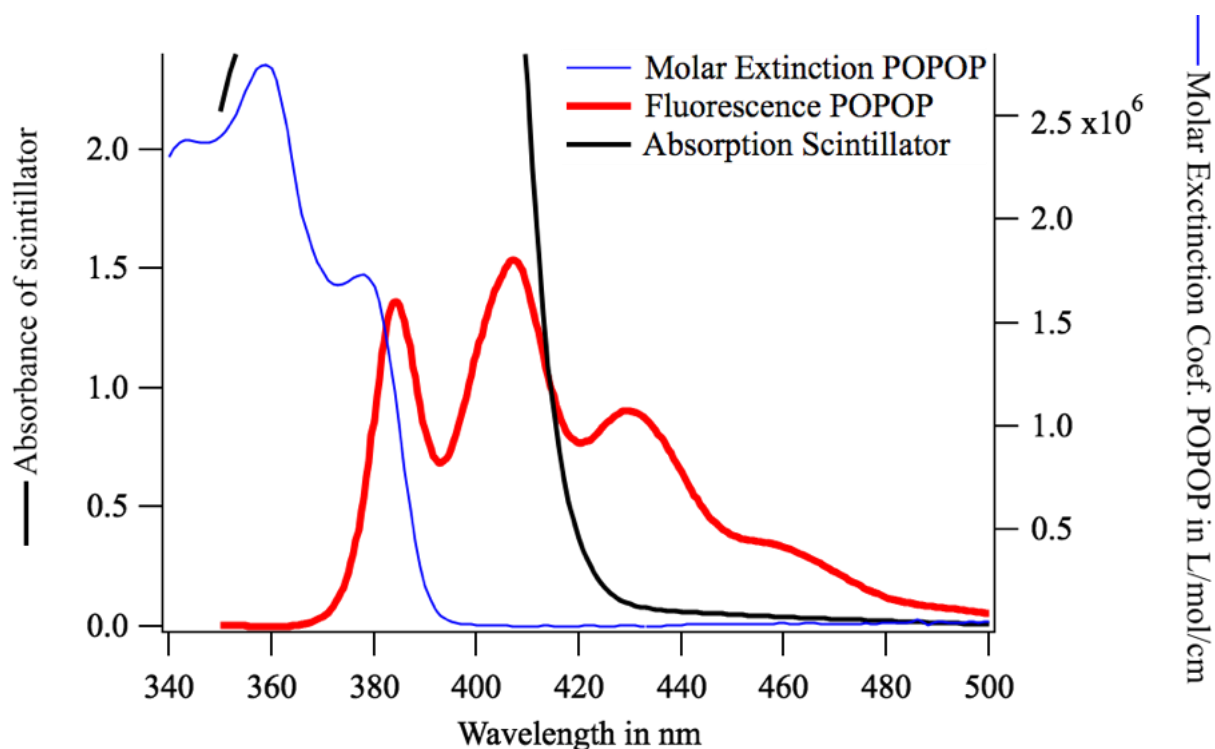


Figure 3. Absorption (blue) and fluorescence (red) spectra of POPOP in cyclohexane from <https://omlc.org/spectra/PhotochemCAD/html/077.html> compared to the absorption spectrum of a 8.3 cm long scintillator with 0.2 wt% POPOP. The red shift observed in the absorption of the scintillator compared to the diluted POPOP is due to the high concentration ( $5 \cdot 10^{-3}$  mol/L) of POPOP in the scintillator. A significant part of the fluorescence is reabsorbed.

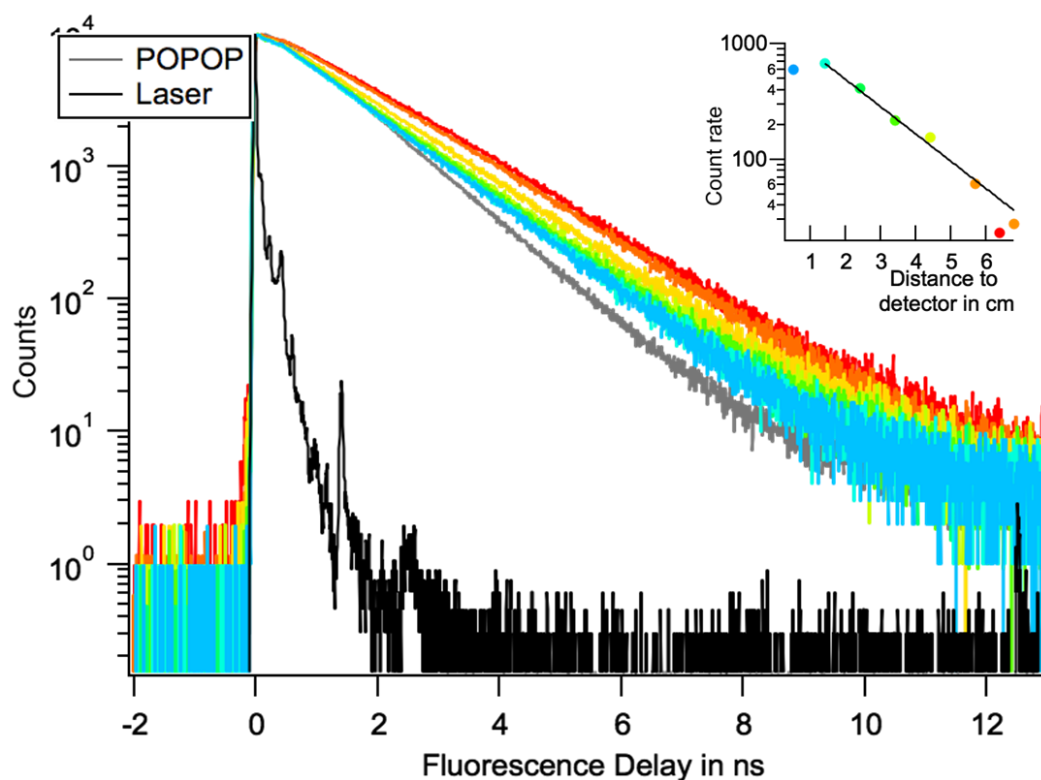


Figure 4. Photoluminescence decay time of the scintillator when excited at various distances from the detector head.

## 2) Influence of the nature of the secondary fluorophore in neutron/gamma discrimination abilities of plastic samples

Lab-made plastic scintillators presented in Table 1 were tested under neutron and gamma rays irradiation thanks to the protocol described above. Fast and slow decays, and the slow relative intensity of each material are listed in Table 2. We already noticed that the FoM value depends on the weight concentration of the secondary fluorophore. When one compares the discriminating efficiency of scintillators loaded with a specific weight concentration of secondary fluorophore, one notices that FoM values are distinct, even considering the associated uncertainty. Besides, we deliberately maximized the total uncertainty associated to the FoM measurement. Therefore, it includes the precision and accuracy errors of the whole detection system, as well as the repeatability and reproducibility uncertainties. Then, the weight concentration also influences the FoM value: when it is 0.2 wt%, FoM increases, except for bis-MSB scintillators. Fast decay times display relatively close values, whereas slow decay times extend from 86 ns up to 126 ns for DMP2 and DPA2, respectively. Furthermore, the slow decay component of Bis2 have not been evaluated because of an unreliable fit: it does not satisfy our fitting criterion, which was in our case  $\chi^2 > 0.99$ .

According to these results, there is a correlation between the FoM value and the slow relative intensity and the slow decay time. Thus, it is not sufficient to have a secondary fluorophore with a slow decay

time like bis-MSB or 9,10-DPA (around a hundred of ns here) but the tail proportion, which would represent the triplet-triplet annihilation, has to be high enough.

Table 2. Fast neutrons/gamma discrimination results (in terms of FoM value) for plastic scintillators ( $\varnothing$  12 mm  $\times$  h 120 mm) presented in Table 1.

Scintillator	$\tau_f$ (ns)	$\tau_s$ (ns)	Slow relative intensity	FoM
Bis1	$11.51 \pm 0.11$	$115 \pm 15$	0.30	$0.51 \pm 0.05$
Bis2	$11.52 \pm 0.13$	Unreliable fit	n.d.	$0.44 \pm 0.04$
DPA1	$17.78 \pm 0.19$	$103 \pm 11$	0.26	$0.58 \pm 0.06$
DPA2	$15.82 \pm 0.17$	$126 \pm 11$	0.29	$0.68 \pm 0.07$
DMP1	$11.59 \pm 0.05$	$88.9 \pm 4$	0.32	$0.60 \pm 0.06$
DMP2	$10.16 \pm 0.05$	$86.2 \pm 3.7$	0.36	$0.72 \pm 0.07$
P1	$11.15 \pm 0.12$	$89.8 \pm 9$	0.30	$0.57 \pm 0.06$
P2	$10.73 \pm 0.16$	$99.7 \pm 12$	0.41	$0.74 \pm 0.07$

If we calculate the ratio of the slow relative intensity and the slow decay time for each tested scintillator, we notice that it follows the FoM trend except for DPA2. Thus, this new criterion measures the efficiency of delayed fluorescence, which is directly correlated to the FoM value. This observation agrees with the results obtained by Dalla Palma *et al.*,<sup>14</sup> who have experimentally observed that the FoM value depends on two parameters. On one side, the light yield is responsible of differences in FoM values, especially at low energies. On the other side, the numerator of Equation 3 is a function of the slow decay intensity. According to our results presented in Figure 5, it should be the ratio of this slow intensity and the slow decay time.

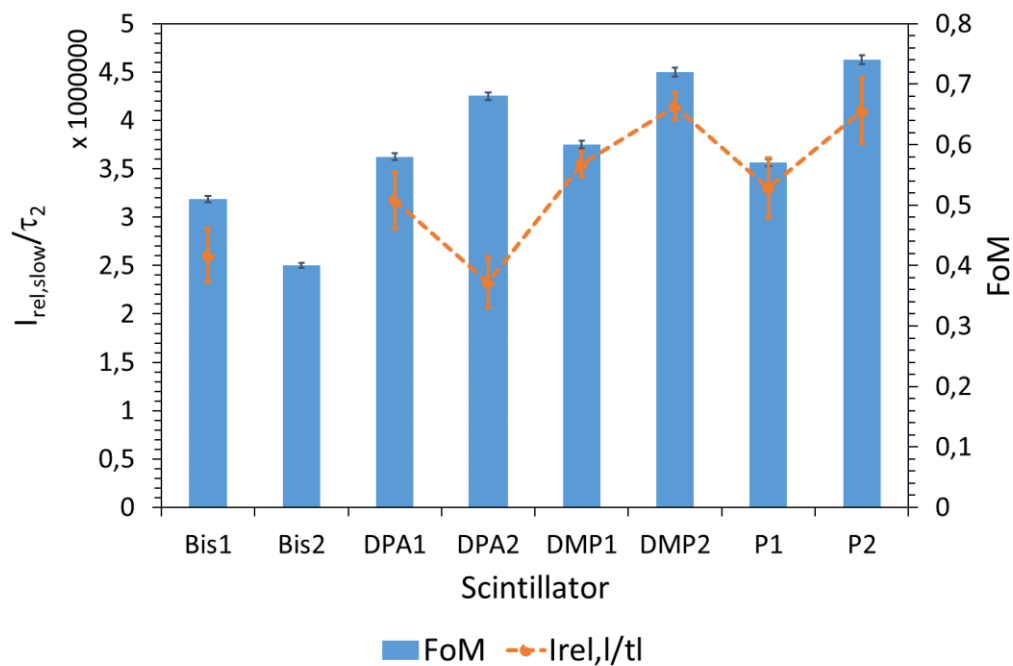


Figure 5. Ratio of the slow relative intensity and the slow decay time depending on the FoM value for each scintillator.

As suspected, the secondary fluorophore plays a role outside its primary role of wavelength shifter. It influences the plastic's neutron/gamma discrimination abilities, it lengthens the short-lived decay and it changes the delayed luminescence intensity. The lengthening of the short-lived decay is due to self-absorption process, which occurs even in medium size scintillators (12 cm length in our experiment). In addition to self-absorption, it is important to check about the scale-up of the material. Thermally initiated polymerization may lead to bulk materials with cracks, bubbles or colored centers, especially for large-size scintillators.

To confirm the good homogeneity of PSD-plastics, two other experiments were also performed, where three identical pieces were randomly cut from a bigger scintillator, and another thin-and-long scintillator was cut into four identical pieces, which were benchmarked. The first series was to evaluate the homogeneity of large scintillators. From a 10 cm height and 7 cm diameter scintillator, three pieces were isolated at the same size and volume, which is 2 cm height and 2.7 cm diameter. At first, their light output was evaluated using a  $^{22}\text{Na}$  source. A 17% light output difference was observed between the best and worst scintillator. Then they were strictly compared in terms of fast neutrons/gamma discrimination. Figure 6 gives the n/ $\gamma$  discrimination results of the three samples. Homogeneity problems are dismissed as a potential explanation for the lack of discrimination in large-scale plastic scintillators.

In the second series testing homogeneity, an 8 cm long and 1.8 cm diameter scintillator was cut in four 2 cm long samples. Whereas the four small samples showed an almost identical FoM value (0.80, 0.77, 0.80 and 0.74 in the range 500 – 1000 keVee), a dramatic decrease of the FoM was observed for the full scintillator, with a value of 0.56 only in the same range of energy. The deviation of the gamma spectra was 5.8 % only, therefore claiming a good light output uniformity between the samples. This factor is not the one affecting the FoM decrease with the length of the scintillator.

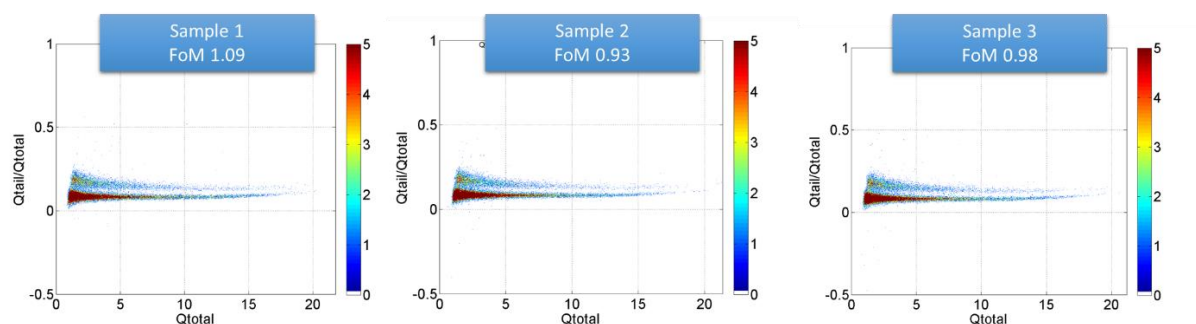


Figure 6. Biparametric spectra and FoM values for 3 randomly cut samples from a bigger monolith.

### 3. Exciplex formation

Beyond reabsorption effects, the secondary fluorophore interacts with the excited state dynamics in the scintillator. If acting only as a wavelength shifter the pulse shapes should reflect the biphenyl excited state dynamics. The pulse shape should be the same whatever the nature of the secondary fluorophore. The differences in the slow component lifetime and fraction that are measured show that the secondary fluorophore plays a role in the excited states nature and dynamics. The slow component is attributed to the triplet-triplet annihilation. In this context, we want to identify the interaction of the triplet state of biphenyl with that of the secondary fluorophore. Herein, only the case of POPOP was studied.

We believe that biphenyl excited states can interact with the secondary fluorophore in two ways:

- Formation of exciplexes (excimers between at least two different molecules),
- Triplet energy transfers between the primary and the secondary fluorophores.

For this experiment, we reproduced the chemical composition of standard lab-made plastic scintillators in the liquid state, and we tested these liquid scintillators by emission spectroscopy. In a few words, exciplexes and excimers are molecular associates, which exist only in excited states, singlet or triplet states according to the excited state of the donor. Their detection is only possible from emission spectroscopy.<sup>15</sup>

329 1) *Exciplex formation*

330 The spectroscopy experiment is carried out in several conditions:

- 331 - The cuvette containing the secondary fluorophore in toluene is put into open air,
- 332 - The same cuvette is continuously degassed with argon,
- 333 - 15 wt% of biphenyl is added to the liquid scintillator. Similarly, the cuvette is put under air and
- 334 argon.

335 Whatever the studied conditions, there was no significant difference in the shape and amplitude of  
336 the emission spectra. We therefore assume that no exciplexes – {primary fluorophore – secondary  
337 fluorophore} or {secondary fluorophore – secondary fluorophore} – were created.

338 The Figure 7 presents the deactivation pathways of the excitation energy in a ternary organic  
339 scintillator. After the ionization by neutrons or gamma rays, the charge recombination creates excited  
340 state of the matrix. This excitation is transferred to the primary and secondary fluorophores by FRET  
341 or Dexter energy transfer. In the neutron-induced traces, the high linear density of charges allows non-  
342 geminated recombinations and the formation of triplet excited states. The presence of these triplet  
343 states is revealed by the delayed luminescence following the triplet-triplet annihilation of densely  
344 excited traces. It is seen that the triplet of the secondary fluorophore is also produced and contributes  
345 as well to the delayed luminescence.

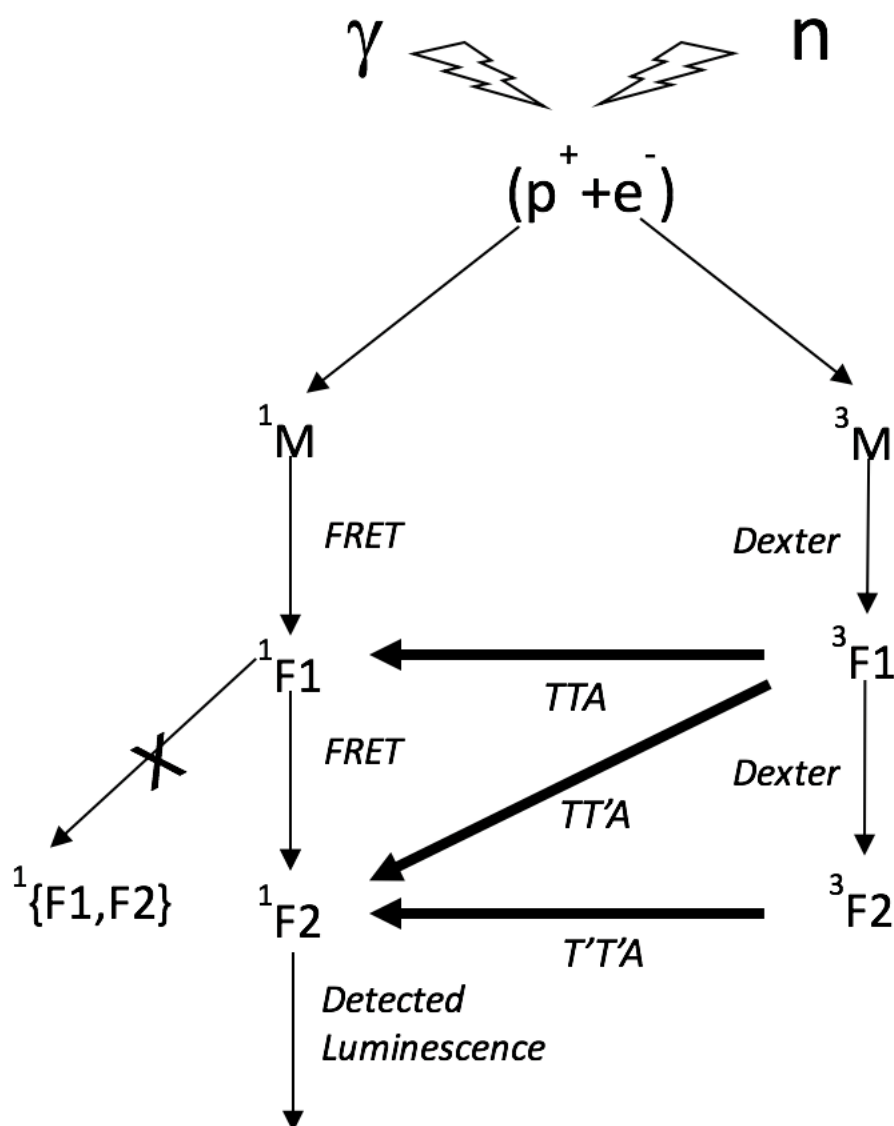


Figure 7. Deactivation pathways of the excitation energy in a ternary organic scintillator. Matrix: M, primary fluorophore: F1 and secondary fluorophore: F2.

## 2) Triplet energy transfers

Triplet state decay times were recorded thanks to a transient absorption experiment. A Nd:YAG laser was used to produce 5 ns pulses. KDP crystals allowed us to quadruple the frequency, thus exciting at the wavelength  $\lambda = 266$  nm. The liquid sample, contained in a 1 cm thick quartz cuvette, was excited with an incident energy of 3 mJ per pulse. Two solutions were studied:

- A = a liquid sample composed with cyclohexane as the matrix, containing  $1.46 \cdot 10^{-3}$  mol.L<sup>-1</sup> biphenyl,
- B = the same A solution plus  $2 \cdot 10^{-4}$  mol.L<sup>-1</sup> POPOP (close to saturation).

In cyclohexane, the laser excitation at 266 nm is absorbed by the biphenyl over a depth of 1 cm. Both transient fluorescence and absorption are recorded; Figure 8 shows the transient absorption and

fluorescence spectroscopy of solution B. Its prompt fluorescence is observed at 430 nm and is followed by a delayed luminescence. The transient absorption at 430 nm rises and reaches a maximum after 2.5  $\mu$ s before decaying. Both transient signals can be identified by their spectra from 380 to 520 nm in Figure 9.

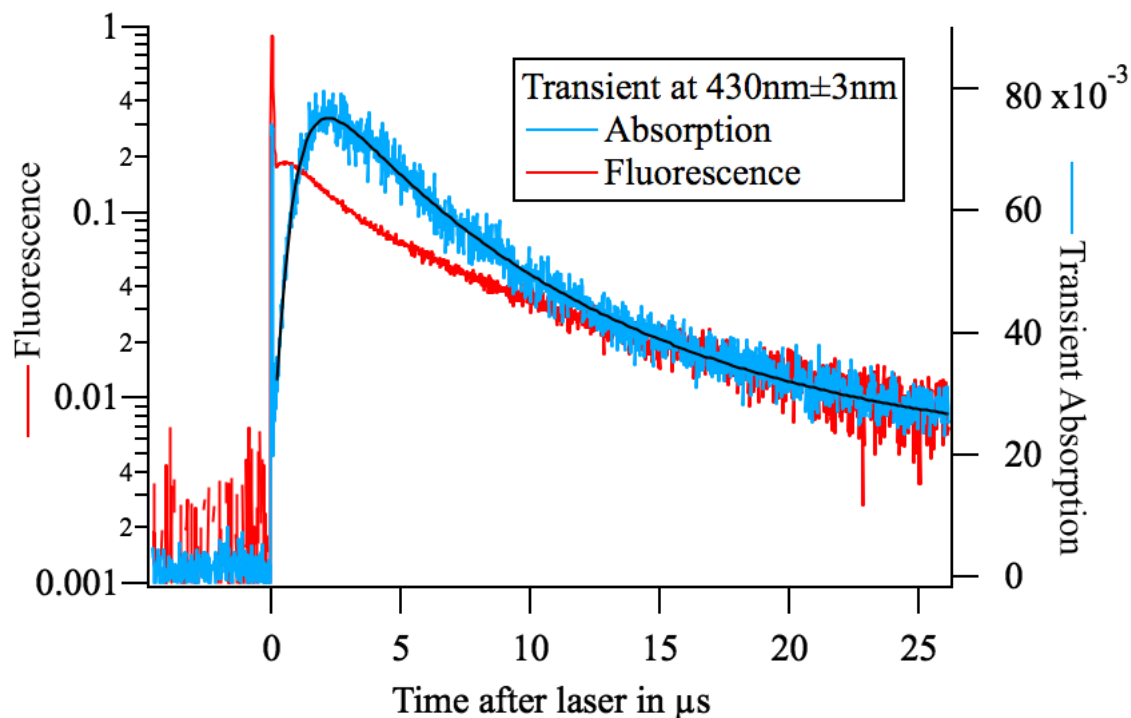


Figure 8. Transient fluorescence (red) and absorption (blue) spectra of solution B made of biphenyl and POPOP in cyclohexane after excitation in the Biphenyl absorption band at 266 nm. Both the prompt and the delayed fluorescence are observed. The POPOP triplet population rises in 2.5  $\mu$ s from the Biphenyl triplet population.

The delayed fluorescence spectrum of solution B (Blue x in Figure 9) shows a major contribution of the POPOP molecule. If one considers the transient absorption spectra, the one of sample A (Red + in Figure 9) shows the influence of biphenyl with a maximum at 370 nm as reported in the literature,<sup>16</sup> whereas the one of sample B (Red x in Figure 9) displays the contribution of POPOP. The global maximum stands at around 500 – 520 nm. Pavlopoulos *et al.* already observed a similar spectrum, and assigned it to the absorption spectrum of the triplet state of POPOP.<sup>17</sup> The rise time of the triplet of POPOP is 0.7  $\mu$ s for a concentration of  $2 \cdot 10^{-4}$  mol.L<sup>-1</sup>. This corresponds to a transfer rate of  $7 \cdot 10^9$  s<sup>-1</sup>, that is close to the diffusion-limited rate. In presence of POPOP, the triplet state of biphenyl transfers to POPOP at any collision.

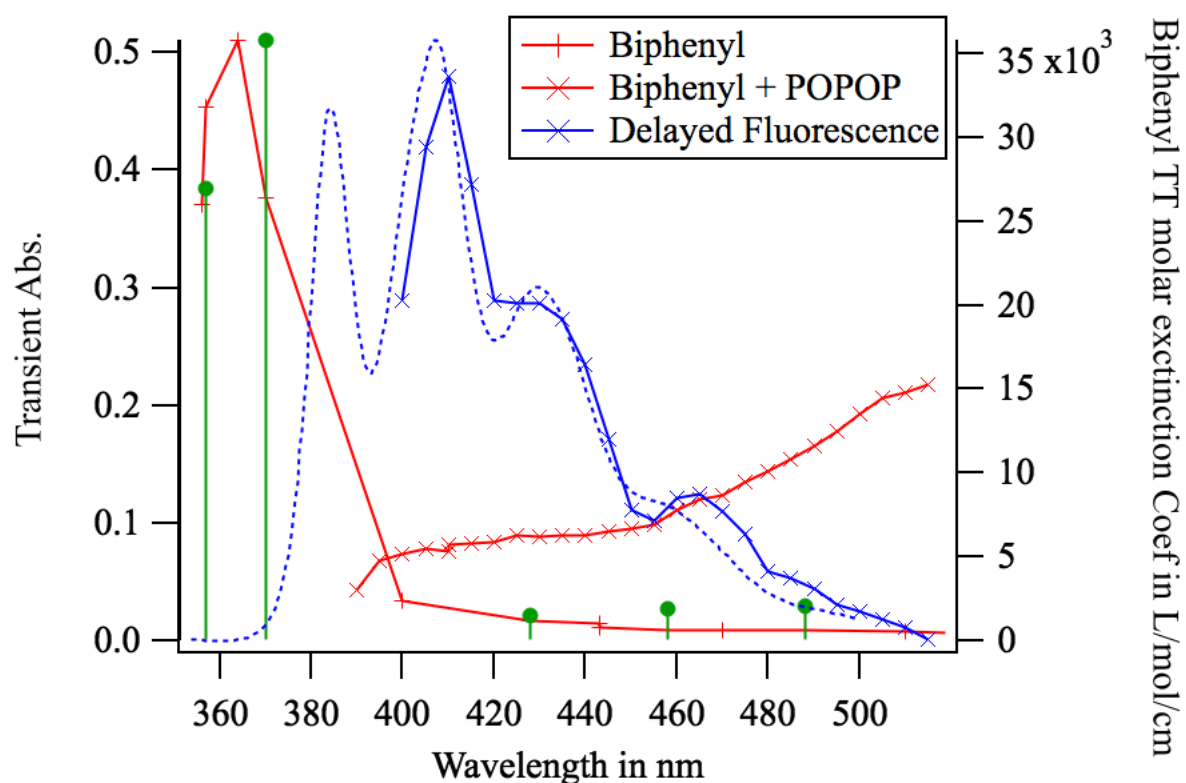


Figure 9. Transient absorption spectra of biphenyl in sample A compares with the published spectrum of biphenyl's triplet (green dots). The transient spectrum of solution B biphenyl + POPOP shows the transfer of triplet state from biphenyl towards POPOP. The delayed fluorescence of POPOP spectrum is compared to the prompt fluorescence one (blue dashed line).

The kinetics of both the POPOP delayed fluorescence and POPOP triplet states are analyzed in Figure 10, which shows that the delayed fluorescence comes from the annihilation of triplet of POPOP through a bimolecular process. Beyond 10  $\mu$ s the delayed fluorescence decays as the square of the POPOP triplet concentration as expected for triplet-triplet annihilation process. At shorter times, the triplet of biphenyl is present and contributes to the delayed luminescence.

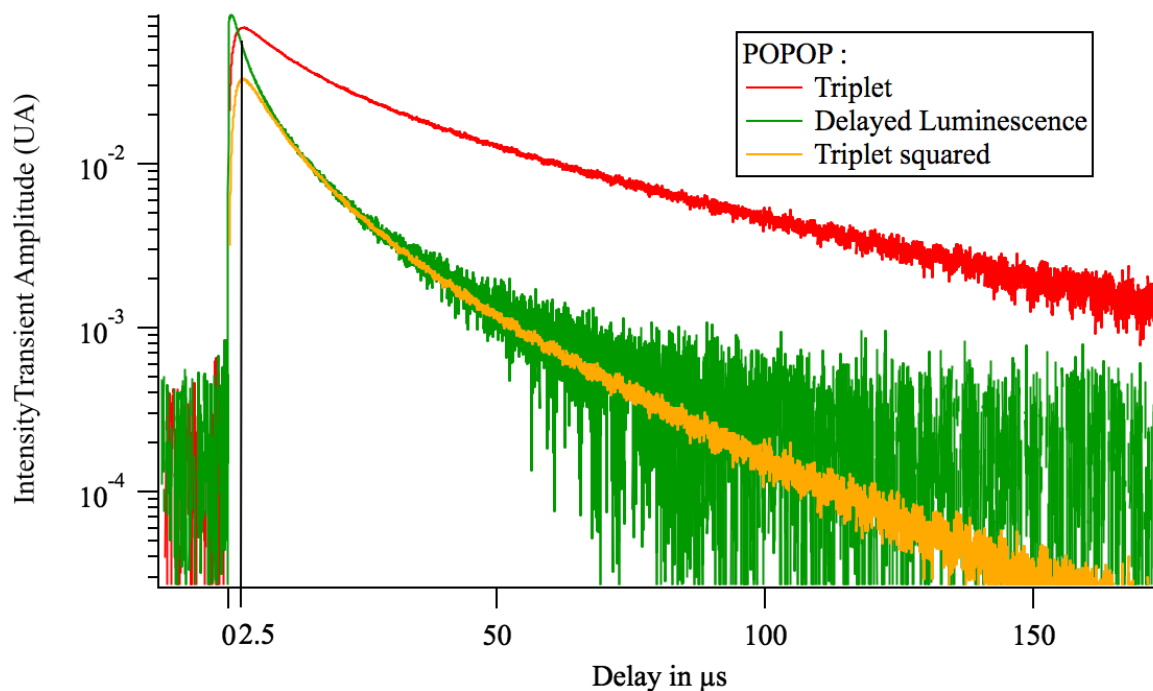
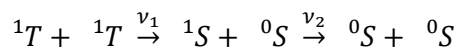


Figure 10. POPOP triplet photoluminescence decay (red), delayed luminescence (green), and squared triplet (orange).

As a reminder, the triplet-triplet annihilation process is written as:

Equation 5



The rate  $\nu_1$  is then:

Equation 6

$$\nu_1 = k_1 [{}^1T]^2$$

The emission of the fluorescence photon is fast (1.2 ns) compared to the triplet-triplet annihilation ( $\mu$ s), then:

Equation 7

$$\nu_1 = \nu_2 = k_1 [{}^1T]^2$$

By definition,  $\nu_2$  refers to a quantity of photons emitted by delayed fluorescence per second, thus corresponds to the delayed fluorescence intensity. According to Equation 7, the intensity of delayed fluorescence is proportional to the square of the excited triplet states concentration in the case of a triplet-triplet annihilation. This is observed in Figure 10, where the tail of the delayed fluorescence is proportional to the square of the POPOP triplet concentration. At shorter times, more fluorescence is observed. However, at times shorter than 2.5  $\mu$ s a rise of POPOP triplet is seen; biphenyl triplet states are present and they contribute to the delayed fluorescence as well. In conclusion, POPOP triplet is present in solution B and triplet-triplet annihilation of POPOP takes place in the liquid sample. At

shorter times TTA between two molecules of the primary fluorophore or between excited molecules of the primary fluorophore and of the secondary fluorophore do occur. In a solid matrix, the triplet of POPOP is trapped because the distance between POPOP molecules (1 nm) is too high to allow hopping. However, the triplet of biphenyl is mobile, which allows biphenyl-biphenyl TTA and biphenyl-POPOP TTA to occur.

#### IV. DISCUSSION

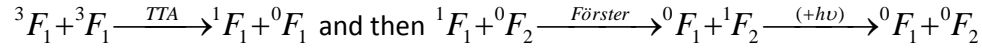
Our work relates the influence of the secondary fluorophore in a ternary plastic scintillator aiming at discriminating fast neutrons from gamma rays. Thanks to neutron/gamma experiments, we showed that the length of POPOP-based plastic scintillators in the range ( $\varnothing$  12 mm  $\times$  h 120 mm) influences negatively the discrimination abilities. We have shown that this is not due to preparation issues where large plastic might be heterogeneous in composition. As self-absorption relies on the spectral overlap between the absorption and the emission spectra of the secondary fluorophore (in a ternary system), we highlight the influence of this fluorophore on neutron/gamma discrimination abilities of the plastic sample. The mean relative loss of FoM is 55 %.

We have shown that scintillators with the same quantity of primary fluorophore, irradiated under the same conditions have different FOM depending on the nature of the secondary fluorophore. The FoM values are quite different despite the identical measurement protocol: it varies from 0.44 for the worse discriminating scintillator (Bis2) to 0.74 for the best one (P2). We have checked if the FoM difference does not come from exciplexes between the primary and the secondary fluorophore in liquid mixtures. Since no exciplex was created in our liquid system (at least with our experimental conditions), we assume that no exciplexes are formed in plastics as well. Thanks to transient absorption experiments, the formation of POPOP triplets was observed when biphenyl was excited. For the first time, the existence of a delayed POPOP luminescence coming from the triplet-triplet annihilation of POPOP was observed as well in a liquid sample. In solid samples, we then assumed that TTA also takes place in plastic scintillators, as well as in liquids. For now, transient absorption measurements have not assessed with accuracy the nature of the involved molecules in the TTA process.

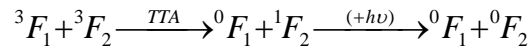
Equations 8 and 9 give the energetic transfers that we observed thanks to transient absorption experiments. This explains the influence of the secondary fluorophore in neutron/gamma discrimination. Equation 8 formalizes the TTA process between two excited triplet states of the primary fluorophore followed by a Förster energy transfer of the resulting excited singlet state of the primary fluorophore towards the secondary fluorophore. Equation 9 relates to a crossed TTA, that is to say

between the excited triplet states of the primary and the secondary fluorophores. These two equations require a diffusion of the biphenyl triplets that can be achieved in solids sample thanks to a hopping of the triplets between biphenyl neighbors. This is in good agreement with the huge increase of primary fluorophores concentration necessary to reach a visible PSD in plastics,<sup>3</sup> along with the observation that plastics loaded with 0.2 wt% secondary fluorophores give better FoM values than 0.1 wt% ones, at least with our global formulation suitable for n/γ PSD (this work).

Equation 8



Equation 9



## V. CONCLUSION

Plastic scintillators aiming at discriminating fast neutrons from gamma rays suffer from a decrease of their performances while increasing their volume. It was proven that fabrication process does not lead to heterogeneous materials, so our main hypothesis is that self-absorption is the main nefarious effect. In particular, the nature and the concentration of the secondary fluorophore have a strong influence on the n/γ discrimination ability, as confirmed from the study of four different molecules. Preliminary experiments seem to highlight specific energy transfers between primary and secondary fluorophores. Future work will consist in assigning probabilities of each transfer, which means evaluating reaction rate constants.

## VI. ACKNOWLEDGEMENTS

We are indebted to the French National Agency “ANR” for financial support, within the frame of the Nessyned project (ANR-15-CE39-0006).

## VII. REFERENCES

- 
- <sup>1</sup> R.T. Kouzes, J.H. Ely, L.E. Erikson, W.J. Kernan, A.T. Lintereur, E.R. Siciliano, D.L. Stephens, D.C. Stromswold, R.M. Van Ginhoven, M.L. Woodring, Neutron detection alternatives to  $^3\text{He}$  for national security applications, *Nucl. Instr. Methods A*, 623 (2010) 1035-1045.
- <sup>2</sup> P. Peerani, A. Tomanin, S. Pozzi, J. Dolan, E. Miller, M. Flaska, M. Battaglieri, R. De Vita, L. Ficini, G. Ottonello, G. Ricco, G. Dermody, C. Giles, Testing on novel neutron detectors as alternative to  $^3\text{He}$  for security applications, *Nucl. Instr. Methods A*, 696 (2012) 110-120.
- <sup>3</sup> G.H.V. Bertrand, M. Hamel, F. Sguerra, Current Status on Plastic Scintillators Modifications, *Chem. – Eur. J.*, 20 (2014) 15660-15685.
- <sup>4</sup> J. Kalyna, I.J. Taylor, Pulse shape discrimination: an investigation of n- $\gamma$  discrimination with respect to size of liquid scintillator, *Nucl. Instr. Methods*, 88 (1970) 277-287.
- <sup>5</sup> B. Sipp, J.A. Miehe, Fluorescence self-absorption effect and time resolution in scintillation counters, *Nucl. Instr. Methods*, 114 (1974) 255-262.
- <sup>6</sup> M. Moszyński, B. Bengtson, Light pulse shapes from plastic scintillators, *Nucl. Instr. Methods*, 142 (1977) 417-434.
- <sup>7</sup> N.P. Zaitseva, A.M. Glenn, A.N. Mabe, M.L. Carman, C.R. Hurlbut, J.W. Inman, S.A. Payne, Recent developments in plastic scintillators with pulse shape discrimination, *Nucl. Instr. Methods A*, 889 (2018) 97-104.
- <sup>8</sup> E. Montbarbon, M.-N. Amiot, D. Tromson, S. Gaillard, C. Frangville, R. Woo, G.H.V. Bertrand, R.B. Pansu, J.-L. Renaud, M. Hamel, Large irradiation doses can improve the fast neutron/gamma discriminating capability of plastic scintillators, *Phys. Chem. Chem. Phys.*, 19 (2017) 28105-28115.
- <sup>9</sup> A.F. Adadurov, P.N. Zhmurin, V.N. Lebedev, V.D. Titskaya, Optimizing concentration of shifter additive for plastic scintillators of different size, *Nucl. Instr. Methods A*, 599 (2009) 167-170.
- <sup>10</sup> Hamamatsu H11284-MOD (R7724-100 photocathode): <https://www.hamamatsu.com/jp/en/R7724.html>.
- <sup>11</sup> P. Blanc, M. Hamel, C. Dehé-Pittance, L. Rocha, R.B. Pansu, S. Normand, Neutron/gamma pulse shape discrimination in plastic scintillators: preparation and characterization of various compositions, *Nucl. Instr. Methods A*, 750 (2014) 1-11.
- <sup>12</sup> Eljen Technology EJ-276 PSD Plastic Scintillator: <https://eljentechnology.com/products/plastic-scintillators/ej-276>.
- <sup>13</sup> R. Voltz, G. Laustriat, Radioluminescence des milieux organiques I. Étude cinétique, *J. Phys. France*, 29 (1968) 159-166.
- <sup>14</sup> M. Dalla Palma, T. Marchi, S. Carturan, C. Checchia, G. Collazuol, F. Gramegna, N. Daldosso, V. Paterlini, A. Quaranta, M. Cinausero, M. Degerlier, Pulse Shape Discrimination in Polysiloxane-Based Liquid Scintillator, *IEEE Trans. Nucl. Sci.*, 63 (2016) 1608-1615.
- <sup>15</sup> T. Förster, Excimers, *Angew. Chemie Int. Ed.*, 8 (1969) 333-343.
- <sup>16</sup> D. Lavalette, C. Tetreau, Triplet-triplet absorption of biphenyl and related compounds. *Chem. Phys. Lett.* 29 (1974) 204-209.
- <sup>17</sup> T.G. Pavlopoulos, P.R. Hammond, Spectroscopic Studies of Some Laser Dyes, *J. Am. Chem. Soc.*, 96 (1974) 6568-6579.